MODEL OF EFFECT OF HOT GAS INGRESS ON TEMPERATURES OF TURBINE DISCS

J Michael Owen

Department of Mechanical Engineering, University of Bath

Bath, BA2 7AY, UK

J.M.Owen@bath.ac.uk

Hui Tang

Department of Mechanical Engineering, University of Bath

Bath, BA2 7AY, UK

H.Tang2@bath.ac.uk

Gary D. Lock

Department of Mechanical Engineering, University of Bath

Bath, BA2 7AY, UK

G.D.Lock@bath.ac.uk

ABSTRACT

Ingress is the leakage of hot mainstream gas through the rim-seal clearance into the wheel-space between the rotating turbine disc (the rotor) and the adjacent stationary casing (the stator). The high-pressure (HP) rotor is purged by a radial outflow of air from the HP compressor, and this cooling air is also used to reduce ingress. The engine designer needs to predict the stator and rotor temperatures as a function of cooling-flow rate. The sealing effectiveness determines how much air is needed to reduce or prevent ingress; although there are numerous theoretical and experimental papers on the effectiveness of different seal geometries, there are few papers on the effect of ingress on the temperature of the rotating disc. This is an unsolved problem of great practical importance: under high stress, a small increase in metal temperature can significantly reduce operating life.

In this paper, conservation equations and control volumes are used to develop theoretical equations for the exchange of mass, concentration and enthalpy in an adiabatic rotor-stator system when ingress occurs. It is assumed that there are boundary layers on the rotor and stator, separated by an inviscid rotating core, and the fluid entrained from the core into the boundary layer on the rotor is recirculated into that on the stator. The superposed cooling flow protects the rotor surface from the adverse effects of hot-gas ingress, which increases the temperature of the fluid entrained into the rotor boundary layer.

A theoretical model has been developed to predict the relationship between the sealing effectiveness on the stator and the adiabatic effectiveness on the rotor, including the effects of both ingress and frictional heating. The model involves the use of a nondimensional buffer parameter, Ψ, which is related to the relative amount of fluid entrained into the rotor boundary layer. The analysis shows that the cooling flow acts as a buffer, which attenuates the effect of hot gas ingress on the rotor, but frictional heating reduces the buffer effect. The theoretical effectiveness curves are in good agreement with experimental data obtained from a rotor-stator heat-transfer rig, and the results confirm that the buffer effect increases as the sealing effectiveness of the rim seals decreases.

The analysis quantifies the increase in the adiabatic rotor temperature due to direct frictional heating, which is separate from the increase due to the combined effects of the ingress and the indirect frictional heating of the entrained fluid. These combined effects are reduced as Ψ increases, and $\Psi = 1$ at a critical flow rate above which there is no entrained fluid and consequently no indirect heating of the rotor.

The model also challenges the conventional physical interpretation of ingress as, in general, not all the hot gas that enters the rim-seal clearance can penetrate into the wheel-space. The ingress manifests itself through a mixing of enthalpy, which can be exchanged even if no ingested fluid enters the wheel-space.

NOMENCLATURE

a, b	inner and outer radius of rotor
A, B	constants
c	concentration
C_M^*	moment coefficient at $r = b$
c_p	specific heat at constant pressure
$C_{w,o}$	nondimensional flow rate ($= \dot{m}_o/\mu b$)
e_M	constant for moment coefficient
f	correction factor for buffering effect
f_F	correction factor for frictional heating
G_c	seal-clearance ratio ($= s_c/b$)
h	heat transfer coefficient ($= q_r/(T_r - T_{r,ad})$)
H	total enthalpy
H'	enthalpy ignoring work term
k	thermal conductivity

$\dot{m}$	mass flow rate
M_r	frictional moment on rotor from a to r
M_r^*	frictional moment on rotor from a to b
Nu	local Nusselt number ($= q_r r/k(T_r - T_{r,ad})$)
Pr	Prandtl number
q_r	heat flux from rotor to air
r	radius
R	recovery factor
Re_ϕ	rotational Reynolds number ($= \rho\Omega b^2/\mu$)
s_c	seal clearance
t	time
T	temperature
U	resultant velocity
U_{seal}	velocity through seal clearance
V_r	radial component of velocity
V_ϕ	tangential component of velocity
V_z	axial component of velocity
W_r	work term for rotor from a to r
W_r^*	work term for rotor from a to b
x	radius ratio ($= r/b$)
β	swirl ratio in core (=$V_{\phi,core}/\Omega r$)
Γ_c	ratio of discharge coefficients for rim seal
δT	frictional heating temperature correction in ε_{ad}
$\delta_1, \delta_2, \delta_3$	corrections for calculating differences between ε_{ad} and $\varepsilon_{H',r}$
ΔT_F	increase in adiabatic-rotor temperature due to frictional heating
ΔT_B	decrease in adiabatic-rotor temperature due to buffer effect
ε	effectiveness
Φ_o	nondimensional sealing parameter ($= U_{seal}/\Omega b$)
Φ_{min}	minimum sealing parameter to prevent ingress

$\lambda_{T,ent}$	turbulent flow parameter due to entrainment
$\lambda_{T,min}$	minimum turbulent flow parameter to prevent ingress
$\lambda_{T,o}$	turbulent flow parameter based on superposed flow ($= C_{w,o}\mathrm{Re}_{\phi}^{-4/5}$)
$\tau_{\phi,r}$	tangential shear stress on rotor
Ψ	buffer parameter
Ω	angular velocity of rotor

Subscripts

ad	adiabatic
B	buffering
c	concentration
$core$	core
$crit$	critical value
e	egress
ent	entrainment
F	frictional heating
H	total enthalpy
H'	enthalpy neglecting work term
i	ingress
m	mass
M	moment on rotor
min	minimum value to prevent ingress
o	superposed flow
r	rotor
s	stator
t	total values

1. INTRODUCTION

The temperature of gas turbine discs is controlled by bleeding cooling air from the high-pressure compressor into the wheel-space between the turbine disc (referred to here as the rotor) and its adjacent casing

(the stator). The air cools the disc and it also helps to reduce the ingress of hot mainstream gas through the rim-seal clearance (see Fig. 1). The sealing effectiveness is a measure of how much air is needed to prevent or reduce the ingress, and most theoretical and experimental research has focused on determining this effectiveness for a variety of seal geometries. Experimenters usually make concentration measurements to determine the effectiveness, and a comprehensive recent review of this is given by Scobie *et al.* [2].

Although there has been considerable research into the sealing effectiveness, there has been comparatively little research on the effect of ingress on the heat transfer from the rotor, the Nusselt number for which is defined by

$$\mathrm{Nu} \stackrel{\text{def}}{=} \frac{q_r r}{k(T_r - T_{r,ad})} \tag{1.1}$$

where q_r is the heat flux from the rotor to the air, and T_r and $T_{r,ad}$ are the temperature and adiabatic temperature of the rotor respectively. Using the adiabatic temperature ensures that the value of the Nusselt number is invariant with the temperature difference. (The symbol $\stackrel{\text{def}}{=}$ is used to distinguish a definition from an equality, and the definition of those symbols not defined in the text can be found in the Nomenclature.)

It is the object of this paper to derive equations for the adiabatic effectiveness and the adiabatic temperature of the rotor, including the effects of both ingress and frictional heating. Section 2 provides a brief review of relevant research. Section 3 uses boundary-layer theory to quantify the theoretical effects of ingress on the flow structure in the wheel-space and on the concentration in the boundary layers on the rotor and stator; it also includes an effectiveness equation for the rotor. Section 4 derives a theoretical model for the effect of ingress on the enthalpy in the boundary layers for an adiabatic rotor and stator with and without frictional heating. Section 4 also includes equations for the adiabatic effectiveness and the adiabatic temperature of the rotor. Section 5 compares the theoretical effectiveness equations with measurements made in a rotor-stator rig. The conclusions are summarized in Section 6.

2. BRIEF REVIEW OF RELEVANT RESEARCH

As Scobie *et al.* [2] have given a recent and comprehensive review of ingress, only those papers of direct relevance to the effect of heat transfer on ingress are discussed here.

Chew *et al.* [3] described a combined experimental and computational fluid dynamics (CFD) study of the sealing effectiveness on the rotor and stator. Radial distributions of sealing effectiveness for two different sealing flow rates (one sealed, and one with ingress) were computed using a 3D CFD model, and the computations were compared with experimental measurements at four radial locations. For concentration, the results showed

that the rotor effectiveness was higher than that on the stator at most radial locations, and it was concluded that the coolant shields the rotor from the ingested fluid.

Pountney *et al.* [4] determined the effect of ingress on heat transfer to the rotor using transient heat transfer tests in a single-stage gas-turbine rig. A step-change in the temperature of the 'cooling air' was created by a mesh heater, and they used narrow-band thermochromic liquid crystal (TLC) to measure the surface temperature of a polycarbonate rotor. The solution of Fourier's equation for a semi-infinite solid was used to calculate h, the local heat transfer coefficient, and $T_{r,ad}$, the adiabatic temperature of the rotor. The buffer ratio - defined as the ratio of the sealing flow rate when ingress first enters the wheel-space to that when it is first experienced by the rotor - was shown to depend on $\lambda_{T,o}$, the turbulent flow parameter which is defined by

$$\lambda_{T,o} \stackrel{\text{def}}{=} \frac{C_{w,o}}{\mathrm{Re}_\phi{}^{4/5}} \tag{2.1}$$

where $C_{w,o}$ is the nondimensional sealing flow rate and Re_ϕ is the rotational Reynolds number. ($\lambda_{T,o}$ is a parameter that arises from turbulent boundary-layer theory, and a value of 0.22 is associated with the flow rate entrained by a free disc.) The amount of ingress entering the wheel-space was determined from concentration measurements on the stator, and it was shown that significant ingress could occur before it affected the rotor.

Cho *et al.* [5], using the same rig as that of Pountney *et al*. [4], measured the transient surface temperature of the rotor using infra-red sensors instead of TLC. The variation of surface temperature with time was then used as a boundary condition for the numerical solution of Fourier's equation, from which $T_{r,ad}$ was calculated. The effectiveness of two single and two double generic rim seals were compared, and a boundary-layer model - developed by Mear *et al.* [6] – showed good agreement between the theoretical and measured values of the adiabatic effectiveness. (The model in [6] took no account of the frictional effects that are included in the analysis described below.)

Comparisons between the sealing effectiveness determined from concentration measurements on the stator and thermal effectiveness determined from temperature measurements on the rotor are based on the analogy between heat and mass transfer. As solid surfaces are impermeable, the analogy is only valid if the surfaces are also adiabatic, which is the reason why it is necessary to determine $T_{r,ad}$ in the heat transfer tests. The analogy was confirmed by Tian *et al*. [7], who used 3D steady CFD to study the effect of ingress on the distribution of temperature and concentration on both the rotor and stator. They concluded that the adiabatic effectiveness determined from the computed temperatures was consistent with concentration effectiveness.

3. EFFECT OF INGRESS ON FLOW STRUCTURE IN WHEEL-SPACE

3.1 Flow structure

In the following section, concentration differences are used to explain the effect of ingress on the flow structure inside a rotor-stator wheel-space. The subscripts r and s are used below to denote values on the rotor and stator respectively.

Fig. 2 shows the simplified flow structure when ingress occurs in a rotor-stator system with a superposed flow of sealing (and cooling) air. There are boundary layers on the rotor and stator, and the layers are separated by an axisymmetric rotating inviscid core. The Taylor-Proudman theorem (see Childs [8]) shows that there can be no axial gradients of the tangential and axial components of velocity in the core. Consequently, the radial component of velocity must be zero in the core and any radial flow must be confined to the boundary layers on the rotor and stator; however, there can be axial flow between the boundary layers. The radial distribution of the local swirl ratio in the core, β, ensures the balance of mass and momentum in the boundary layers at all radial locations. In general, $\beta = \beta(r)$, and it decreases in magnitude as the superposed flow rate increases. However, even in the absence of ingress, β increases with radius near the shroud.

The superposed flow enters the system through an *inner region* in which all the available fluid is entrained by the boundary layer on the rotor. In the *outer recirculation region*, the fluid entrained by the rotor boundary layer recirculates into the stator boundary layer and the remainder (with a flow rate equal to that of the superposed flow and ingress) leaves the system through the rim seal. In the model discussed below, it is assumed that the egress and ingress are fully mixed before the flow enters the stator boundary layer. It is also assumed that ingress has no significant effect on the flow structure in the wheel-space; this assumption is consistent with the velocity measurements made by Sangan et al. [1].

The inner and outer regions are the sources for the flow in the boundary layers on the rotor and stator respectively, and in the radii between these regions the axial flow is from the stator to the rotor. Importantly, the flow rate of fluid leaving the stator to be entrained into the boundary layer on the rotor decreases as the superposed flow rate increases.

The temperature of the flow down the stator, and consequently that of the axial flow to the rotor, is increased by both the ingress of hot gas and the frictional heating of the rotor. The superposed flow therefore acts as a buffer, which reduces the heating effect of the hot fluid that is entrained into the rotor boundary layer.

3.2 Concentration on stator

An overbar is used below to denote bulk-mean averages, and an asterisk denotes values at $r = b$.

It is assumed here that $c_o < c_i$. It is also assumed that the ingress and egress are fully mixed inside a recirculation region that has no significant radial extent. That is, the mixing occurs at $r = b$.

The mass flow rate entering the wheel-space shown in Fig. 3a is $\dot{m}_o + \dot{m}_i$, and that leaving is $\dot{m}_e$. Conservation of the mass entering and leaving the wheel-space means that

$$\dot{m}_o + \dot{m}_i = \dot{m}_e \tag{3.1}$$

Similarly, for the concentration

$$\dot{m}_o c_o + \dot{m}_i c_i = \dot{m}_e c_e \tag{3.2}$$

As the flow is assumed to be fully mixed at $r = b$ then $c_s = c_e$.

Two definitions of sealing effectiveness are in common use: ε_m is the effectiveness based on mass flow rates and $\varepsilon_{c,s}$ is based on concentration measurements on the stator, where

$$\varepsilon_m \stackrel{\text{def}}{=} \frac{\dot{m}_o}{\dot{m}_e} \tag{3.3}$$

and

$$\varepsilon_{c,s} \stackrel{\text{def}}{=} \frac{c_i - c_s}{c_i - c_o} \tag{3.4}$$

It follows from the above equations that $\varepsilon_{c,s} = \varepsilon_m$.

3.3 Concentration on rotor

Referring to Fig 3b, between a and the radial location r the mass flow rate entering the control volume is $\dot{m}_o + \dot{m}_s$ and that leaving is $\dot{m}_r$.

The mass flow rate in the rotor boundary layer is given by

$$\dot{m}_r = \dot{m}_o + \dot{m}_{ent} \tag{3.5a}$$

where $\dot{m}_{ent}$, the flow rate entrained into the rotor boundary layer, is given by

$$\dot{m}_{ent} = \dot{m}_s \tag{3.5b}$$

At $r = b$, there is a discontinuity between the equations for the inner and outer control volumes: in general, as $\dot{m}^*_{ent}$ depends on the swirl ratio in the wheel-space, $\dot{m}_s{}^*$ is *not* equal to $\dot{m}_i$. (This was also shown by the boundary-layer analysis of Mear-Stone [9].) In effect, the interface at $r = b$ can be thought of as an imaginary cylindrical membrane or an orifice ring, a device used by Owen [10,11] to predict ingress and egress through rim seals by the assumption of a discontinuity in pressure across the membrane. (This device is also analogous to the actuator-disc theory used in fluid mechanics text books - see, for example, White [12] - to calculate the efficiency of propellers and wind turbines.) *In practice, it means that not all the hot gas that enters the rim-seal clearance*

necessarily penetrates into the wheel-space: the concentration inside the wheel-space can be changed even if no ingested fluid enters the wheel-space.

For $r < b$, as no fluid enters the stator boundary layer, and as the flow is assumed to be fully mixed, the concentration cannot change and so c_s must be invariant with radius and must equal the value in the core. (This is consistent with the experimental measurements described in [2].) As $c_s \geq c_o$, the entrained fluid increases the concentration in the rotor boundary layer, so that

$$\dot{m}_r \bar{c}_r = \dot{m}_o c_o + \dot{m}_s c_s \tag{3.6}$$

Unlike the stator boundary layer, in which the fluid is a fully mixed and $c_s = c_s^* = constant$, in the rotor boundary layer $\bar{c}_r$ changes with radius; the overbar is used to denote the bulk-average value of the mixture of the superposed and entrained fluid.

It follows from eqs (3.5a) and (3.6) that

$$c_s - \bar{c}_r = \frac{\dot{m}_o}{\dot{m}_r}(c_s - c_o) \tag{3.7}$$

By analogy with eq (3.7) it is assumed that

$$c_s - c_r = \Psi\,(c_s - c_o) \tag{3.8}$$

where

$$\Psi \stackrel{\text{def}}{=} f\frac{\dot{m}_o}{\dot{m}_r} \tag{3.9}$$

Ψ can be thought of as a buffer parameter that helps to shield the rotor from the effect of ingress, and f is an empirical constant that relates c_r to $\bar{c}_r$. It should be noted that $0 \leq \Psi \leq 1$.

A concentration effectiveness for the rotor, similar to that for the stator, can be defined as

$$\varepsilon_{c,r} \stackrel{\text{def}}{=} \frac{c_i - c_r}{c_i - c_o} \tag{3.10}$$

It follows from eq. (3.4), (3.8) and (3.10) that

$$\varepsilon_{c,r} = \varepsilon_{c,s} + \Psi[1 - \varepsilon_{c,s}] \tag{3.11}$$

It should be noted that $\varepsilon_{c,r} = 1$ if either $\varepsilon_{c,s} = 1$ or $\Psi = 1$. As Ψ is proportional to $\dot{m}_o$, there is a critical flow rate at which $\Psi = 1$; above this flow rate, $\varepsilon_{c,r} = 1$ even if $\varepsilon_{c,s} < 1$. Experimental evidence for this is given in Section 5.

4. EFFECT OF INGRESS ON TEMPERATURE IN WHEEL-SPACE

For the steady-flow energy equation it is necessary to use the total enthalpy, H, where

$$H = c_p T + \frac{1}{2} U^2 \tag{4.1}$$

U being the resultant velocity. As $V_\phi^2 \gg V_r^2 \gg V_z^2$ in rotor-stator systems,

$$U^2 \approx V_\phi^2 \tag{4.2}$$

The control volumes for enthalpy are shown in Fig. 4.

4.1 Adiabatic effectiveness, neglecting frictional effects

4.1.1 Adiabatic effectiveness of stator, neglecting frictional effects

A prime is used below to denote that the values do not include frictional effects.

For an adiabatic system in the absence of frictional heating, the conservation equations for enthalpy are equivalent to those for concentration given in Section 3, so that

$$\dot{m}_o H_o + \dot{m}_i H_i = (\dot{m}_o + \dot{m}_i) H_e' \tag{4.3}$$

For fully mixed flow, $H_s' = H_e'$. In engines, $H_i > H_o$, so $H_o \leq H_s{}' \leq H_i$.

The adiabatic effectiveness of the stator is defined as

$$\varepsilon_{H',s} \stackrel{\text{def}}{=} \frac{H_i - H_s'}{H_i - H_o} \tag{4.4}$$

It follows that $\varepsilon_{H',s} = \varepsilon_m = \varepsilon_{c,s}$.

4.1.2 Adiabatic effectiveness of rotor, neglecting frictional effects

In an adiabatic system, if the frictional heating is not significant, there is similarity between the distribution of concentration and enthalpy inside the boundary layers. The equivalent to eq (3.6) is

$$\dot{m}_o H_o + \dot{m}_s H_s' = \dot{m}_r \bar{H}_r' \tag{4.5}$$

Using the same arguments used for concentration, it follows by analogy with eq (3.11) that

$$\varepsilon_{H',r} = \varepsilon_{c,s} + \Psi[1 - \varepsilon_{c,s}] \tag{4.6}$$

As discussed below, this result will be modified by the effect of frictional heating.

4.2 Adiabatic effectiveness, including frictional effects

Frictional heating means that the frictional moment, M_r, on the rotor creates a work term, W_r, in the boundary layer, and the adiabatic-rotor temperature will be increased. It follows

$$W_r = M_r \Omega \tag{4.7}$$

and

$$M_r = -2\pi \int_a^r r^2 \tau_{\phi,r} dr \tag{4.8}$$

where the tangential shear stress on the rotor is negative.

Although there is no work done on the stator, the temperature of the fluid recirculated from the rotor boundary layer at $r = b$ is increased by work done on the rotor. Consequently, as shown below, $H_s > H_s'$.

4.2.1 Adiabatic effectiveness of stator, including frictional effects

Referring to Fig. 4a, if $\dot{m}_o \leq \dot{m}_r$, eq (4.3) for the stator becomes

$$\dot{m}_o H_o + \dot{m}_i H_i + W_r^* = (\dot{m}_o + \dot{m}_i) H_s \tag{4.9}$$

where W_r^* is the work done by the rotor on the air between $r = a$ and $r = b$. It can be shown that $H_s > H_s'$ and that

$$H_s - H_o = \varepsilon_{c,s} \frac{W_r^*}{\dot{m}_o} + (H_i - H_o)(1 - \varepsilon_{c,s}) \tag{4.10}$$

It should be noted that, as no work is done by the stator, H_s (like the concentration) is invariant with radius.

By analogy with eq (4.4), the adiabatic effectiveness for the stator is defined as

$$\varepsilon_{H,s} \stackrel{\text{def}}{=} \frac{H_i - H_s}{H_i - H_o} \tag{4.11}$$

and it follows from eq (4.9) that

$$\varepsilon_{H,s} = \varepsilon_{c,s}[1 - \frac{W_r^*}{\dot{m}_o (H_i - H_o)}] \tag{4.12}$$

4.2.2 Adiabatic effectiveness of rotor, including frictional effects

Referring to Fig. 4b, if $\dot{m}_o \leq \dot{m}_r$, eq (4.5) for the rotor at radius *r* becomes

$$\dot{m}_o H_o + \dot{m}_s H_s + W_r = \dot{m}_r \bar{H}_r \tag{4.13}$$

which can be rewritten as

$$\bar{H}_r - H_s = \frac{W_r}{\dot{m}_r} - \frac{\dot{m}_o}{\dot{m}_r}(H_s - H_o) \tag{4.14}$$

where W_r is the work done by the rotor between the radii a and r, and $H_s - H_o$ is given by eq (4.10). The first term on the right hand side represents the frictional heating of the rotor between *a* and *r*. The second term represents the entrainment of enthalpy from the core into the rotor boundary layer; $\dot{m}_o$ creates the buffering effect, which helps to shield the rotor from the adverse effect of the entrained fluid.

Using the subscripts F and B to denote frictional heating and buffering respectively, it is assumed that

$$\bar{H}_r - H_s = (\bar{H}_r - H_s)_F + (\bar{H}_r - H_s)_B \tag{4.15}$$

where

$$(\bar{H}_r - H_s)_F = \frac{W_r}{\dot{m}_r} \tag{4.16}$$

and

$$(\bar{H}_r - H_s)_B = -\frac{\dot{m}_o}{\dot{m}_r}(H_s - H_o) \tag{4.17}$$

H_r can replace $\overline{H}_r$ in eq (4.16) using the empirical factor f_F, so that

$$(H_r - H_s)_F = f_F \frac{W_r}{\dot{m}_r} \tag{4.18}$$

Although W_r and f_F could be solved from the boundary layer equations, a simpler approach is to use the result obtained by Owen & Rogers [8]. In the absence of ingress, they used the Reynolds analogy between angular momentum and enthalpy to show that the adiabatic rotor temperature is given by

$$T_{r,ad,F} - T_{core} = R\frac{\Omega^2 r^2}{2c_p}(1-\beta)^2 \tag{4.19}$$

where $T_{r,ad,F}$ is the adiabatic rotor temperature determined only by frictional heating, T_{core} is the temperature in the core and R is a recovery factor; it is usually assumed that $R = \mathrm{Pr}^{1/3}$. Therefore

$$(H_r - H_s)_F = c_p T_{r,ad,F} + \frac{1}{2}\Omega^2 r^2 - c_p T_{core} - \frac{1}{2}\beta^2\Omega^2 r^2 = \frac{\Omega^2 r^2}{2}[R(1-\beta)^2 + (1-\beta^2)] \tag{4.20}$$

where H_s is given by eq (4.9).

In the absence of frictional effects, it is assumed by analogy with eq (3.8) that

$$(H_r - H_s)_B = -\Psi(H_s - H_o) \tag{4.21}$$

It follows from eq. (4.20) and (4.21) that

$$H_r - H_s = \frac{\Omega^2 r^2}{2}[R(1-\beta)^2 + (1-\beta^2)] - \Psi(H_s - H_o) \tag{4.22}$$

An adiabatic effectiveness for rotor when the frictional heating is included can be defined

$$\varepsilon_{H,r} \stackrel{\text{def}}{\equiv} \frac{H_i - H_r}{H_i - H_o} = 1 - \frac{H_s - H_o}{H_i - H_o} - \frac{H_r - H_s}{H_i - H_o} \tag{4.23}$$

Using eqs (4.10) and (4.22), it follows that

$$\varepsilon_{H,r} = \varepsilon_{c,s} + \Psi\left(1 - \varepsilon_{c,s}\right) - \varepsilon_{c,s}(1-\Psi)\frac{W_r^*}{\dot{m}_o(H_i - H_o)} - \frac{\Omega^2 r^2}{2(H_i - H_o)}[R(1-\beta)^2 + (1-\beta^2)] \tag{4.24a}$$

Alternatively,

$$\varepsilon_{H,r} = \varepsilon_{H',r} - \varepsilon_{c,s}(1-\Psi)\frac{W_r^*}{\dot{m}_o(H_i - H_o)} - \frac{\Omega^2 r^2}{2(H_i - H_o)}[R(1-\beta)^2 + (1-\beta^2)] \tag{4.24b}$$

The first term on the right hand side of eq (4.24b) is the adiabatic effectiveness neglecting frictional effects; the second term is caused by the indirect frictional heating of the rotor due to the recirculated fluid; the third term is caused by the direct frictional heating of the rotor.

It is shown in eq (A6) in Appendix A that

$$\frac{W_r^*}{\dot{m}_o(H_i - H_o)} = \frac{e_M}{\lambda_{T,o}} \frac{\Omega^2 b^2}{2(H_i - H_o)} \tag{4.25}$$

where e_M is a constant that depends on the swirl ratio, β. So eq (4.24b) can be written as

$$\varepsilon_{H,r} = \varepsilon_{H',r} - \varepsilon_{c,s}(1 - \Psi) \frac{e_M}{\lambda_{T,o}} \frac{\Omega^2 b^2}{2(H_i - H_o)} - \frac{\Omega^2 r^2}{2(H_i - H_o)} [R(1 - \beta)^2 + (1 - \beta^2)] \tag{4.26}$$

4.2.3 Adiabatic rotor temperature due to frictional heating and ingress

Eq (4.22) can be rewritten in terms of $T_{r,ad}$ and T_s as

$$T_{r,ad} - T_s = R \frac{\Omega^2 r^2}{2c_p} (1 - \beta)^2 - \frac{\Psi}{c_p} (H_s - H_o) \tag{4.27}$$

It follows from eq (4.10) and (4.25) that

$$T_{r,ad} - T_s = R \frac{\Omega^2 r^2}{2c_p} (1 - \beta)^2 - \frac{\Psi}{c_p} \left[\varepsilon_{c,s} \frac{e_M}{\lambda_{T,o}} \frac{\Omega^2 b^2}{2} + (H_i - H_o)(1 - \varepsilon_{c,s}) \right] \tag{4.28}$$

It is useful to express eq (4.28) in terms of the inlet total temperature, $T_{o,t}$, instead of T_s. This can be done using eq (4.22), which is rewritten as

$$H_r - H_o = \frac{\Omega^2 r^2}{2} [R(1 - \beta)^2 + (1 - \beta^2)] + (1 - \Psi)(H_s - H_o) \tag{4.29}$$

or in terms $T_{r,ad}$ and $T_{o,t}$ (the total temperature of the superposed flow) as

$$T_{r,ad} - T_{o,t} = \frac{\Omega^2 r^2}{2c_p} [R(1 - \beta)^2 - \beta^2] + \frac{1 - \Psi}{c_p} (H_s - H_o) \tag{4.30}$$

It follows from eqs (4.10) and (4.25) that

$$T_{r,ad} - T_{o,t} = \frac{\Omega^2 r^2}{2c_p} [R(1 - \beta)^2 - \beta^2] + \frac{1 - \Psi}{c_p} \left[\varepsilon_{c,s} \frac{e_M}{\lambda_{T,o}} \frac{\Omega^2 b^2}{2} + (H_i - H_o)(1 - \varepsilon_{c,s}) \right] \tag{4.31}$$

The first term on the right-hand-side of eq (4.31) is the direct increase in the adiabatic rotor temperature due to direct frictional heating. The second term is the increase due to the combined effects of the ingress and the indirect frictional heating of the recirculating fluid, both of which are reduced as Ψ increases. As stated in Section 3, Ψ = 1 at a critical flow rate above which there is no entrainment and consequently no indirect heating of the rotor.

In gas turbines, the increase of rotor temperature due to the direct frictional heating can be as high as 40C, which can have a significant effect on the stress and fatigue life of this expensive component. The buffer effect helps to offset the adverse effects of both ingress and the indirect frictional heating.

5. COMPARISON BETWEEN THEORY AND EXPERIMENTS

5.1 Experimental measurements

The experimental rig, instrumentation and data analysis are described in detail by Cho et al [5] so only the salient features relevant to this paper are described here.

Fig. 5 shows the rotor-stator rig and instrumentation used in the experiments. To achieve quasi-adiabatic surfaces, the rotor and stator were each covered by a 5-mm-thick sheet of Rohacell insulating foam ($k \approx 0.03\mathrm{W/mK}$). The rotor, which was 380 mm in diameter, could be rotated at speeds up to 4000 rpm, providing a maximum rotational Reynolds number of $\mathrm{Re}_\phi = 1.1 \times 10^6$. The seal geometries used in the tests are shown in Fig. 6; clearance s_c = 2 mm for both seals and other dimensions are given in [5].

In the concentration tests, 1% of carbon dioxide was injected into the unheated superposed flow, and the concentration was monitored at 15 radial positions on the stator. The definition of the concentration effectiveness, $\varepsilon_{c,s}$, was equivalent to that used in eq (3.4).

In the heated tests, the superposed flow was heated by a mesh heater, which produced a step-change in temperature of around 30 ℃ at inlet to the wheel-space. The transient temperature of the rotor was measured at two radial locations (r/b = 0.81 and 0.937) by infra-red sensors, and the air temperature in the core was measured by fast-response thermocouples.

The authors solved Fourier's 1D equation for the quasi-adiabatic rotor to determine the steady-state values (as $t \to \infty$) of $T_{r,ad}$ and $\tilde{T}_{r,ad}$, the adiabatic rotor temperature with and without ingress respectively. ($\tilde{T}_{r,ad}$ is equal to the total temperature of the superposed flow, $T_{o,t}$, plus a small degree (~ 1C) of frictional heating at the given radial position.) The authors defined their adiabatic effectiveness, ε_{ad}, by

$$\varepsilon_{ad} = \frac{T_{r,ad} - T_{i,t}}{\tilde{T}_{r,ad} - T_{i,t}} \tag{5.1}$$

where $T_{i,t}$ is the total temperature of the air measured by a thermocouple in the annulus. As discussed in Appendix B, $\varepsilon_{ad} \approx \varepsilon_{H',r}$ in these experiments.

5.2 Comparison with experimental data

Fig. 7 shows comparisons between the measured and theoretical variations of effectiveness for tests with the two single seals. The concentration measurements were correlated using the effectiveness equation for externally-induced ingress [13]:

$$\frac{\Phi_o}{\Phi_{min}} = \frac{\varepsilon_{c,s}}{[1 + \Gamma_c^{-\frac{2}{3}}(1 - \varepsilon_{c,s})^{\frac{2}{3}}]^{3/2}} \tag{5.2}$$

where Φ_o, the *inviscid* sealing flow parameter is defined as:

$$\Phi_o \stackrel{\text{def}}{=} \frac{U_{seal}}{\Omega\, b} = \frac{C_{w,o}}{2\pi G_c \mathrm{Re}_\phi} \tag{5.3}$$

where U_{seal} is the velocity through the rim-seal clearance, Φ_{min} is the minimum value of Φ_o needed to prevent ingress, Γ_c is the ratio of the discharge coefficients for ingress and egress, and other symbols are defined in the Nomenclature. It can be shown that Φ_o is related to $\lambda_{T,o}$, the turbulent flow parameter defined in eq (2.1), by

$$\lambda_{T,o} = 2\pi G_c \mathrm{Re}_\phi^{0.2} \Phi_o \tag{5.4}$$

Coincidently, for the experiments discussed here (where $Re_\phi \approx 10^6$ and $G_c = 0.0105$), $\lambda_{T,o} \approx \Phi_o$.

Eq (3.9) for the buffer parameter is written below as

$$\Psi = f \frac{\dot{m}_o}{\dot{m}_o + \dot{m}_{ent}} \tag{5.5}$$

which can be expressed in terms of $\lambda_{T,o}$ by

$$\Psi = f \frac{\lambda_{T,o}}{\lambda_{T,o} + \lambda_{T,ent}} \tag{5.6}$$

As the entrained flow rate is a maximum when $\lambda_{T,o}$ = 0 and reduces as $\lambda_{T,o}$ increases, it is assumed here that

$$\lambda_{T,ent} = A\, e^{-B\lambda_{T,\mathrm{o}}} \tag{5.7}$$

where A and B are empirical constants. As nothing is known about the constant f, it is assumed for simplicity that $f = 1$. It follows that eq (5.5) can be approximated by

$$\Psi = \frac{\lambda_{T,0}}{\lambda_{T,0} + A\, e^{-B\lambda_{T,0}}} \approx \frac{\Phi_0}{\Phi_0 + A\, e^{-B\Phi_0}} \tag{5.8}$$

where the constants A and B are chosen to give the best statistical fit to the values of $\varepsilon_{H',r}$ determined from the experimental measurements.

Fig. 7 show the experimental values together with the fitted curves of $\varepsilon_{H',r}$ and $\varepsilon_{c,s}$ versus Φ_0 for the two seals shown in Fig. 6: $\varepsilon_{c,s}$ was fitted by Cho et al. [5] using eq (5.2); $\varepsilon_{H',r}$ was fitted here using eq (4.6), which is rewritten below for convenience as

$$\varepsilon_{H',r} = \varepsilon_{c,s} + \Psi[1 - \varepsilon_{c,s}] \tag{5.9}$$

where eq (5.8) was used to determine the variation of Ψ with Φ_0. The constants Γ_c, Φ_{min} , A and B used in these correlations are shown in Table 1, and the variation of Ψ with Φ_0 corresponding to these values of A and B is shown in Fig. 8.

It should be pointed out that Fig. 7 looks very similar to Fig. 13 of [5]. In fact the curves for $\varepsilon_{c,s}$ are identical as they were based on the correlations of those authors (see eq. 5.2). However the curves for $\varepsilon_{H',r}$ are different as they were based on the equation for Ψ given in eq (5.8). As the values of A and B shown in Table 1 are the same for both seals, Ψ does not depend on the seal geometry. Eq (5.9) shows that the values of $\varepsilon_{H',r}$ – which depend on $\varepsilon_{c,s}$ - are seal dependent.

As noted in Section 3, there is a critical flow rate at which $\Psi = 1$ and $\varepsilon_{H',r} = \varepsilon_{c,s}$; above this flow rate, $\varepsilon_{H',r} = 1$ even if $\varepsilon_{c,s} < 1$. This implies that there is also a critical value of $\lambda_{T,o}$, but the exponential approximation used in eq (5.7) means that $\Psi \to 1$ as $\lambda_{T,o} \to \infty$. It is therefore convenient to use a limit close to unity, $\Psi = 0.99$, say, for which $\lambda_{T,o,crit} \approx \Phi_{o,crit} \approx 0.143$ is the critical value for these two seals. Table 1 shows that $\Phi_{min} > \Phi_{o,crit}$ for the axial-clearance seal, and Fig. 7a shows that there is a significant buffering effect (where $\varepsilon_{H',r} > \varepsilon_{c,s}$) at all flow rates for this seal. However, $\Phi_{min} < \Phi_{0,crit}$ for the radial-clearance seal, and Fig. 7b shows that the buffering effect is significantly reduced. It follows that, in general, the buffering effect will increase as the seal effectiveness decreases.

6. CONCLUSIONS

The principal assumption in the theoretical model is that there are boundary layers on the rotor and stator, separated by an inviscid rotating core, and that ingress has no significant effect on the flow structure inside the wheel-space. It is also assumed that the flow is fully-mixed before it enters the wheel-space, and consequently the concentration and enthalpy inside the stator boundary layer are invariant with radius and are equal to the values in the core. Based on these assumptions, control-volume analysis and a version of actuator-disc theory system has been used to derive equations for the effect of ingress on the concentration and enthalpy inside the boundary layers of an adiabatic rotor-stator system, with and without the effect of frictional heating. The resulting equations for the adiabatic temperature and effectiveness of the rotor involve an empirical buffer parameter, Ψ, which depends on the rate of entrainment of fluid into the rotor boundary layer.

The ‘frictionless model’ model has been validated using published measurements made in a quasi-adiabatic rotor-stator rig in which concentration and temperature measurements were used to determine the

effectiveness for the stator and rotor respectively. The buffer parameter, Ψ, which was determined from a single statistical fit of the data obtained for two different rim seals, was used to determine the rotor effectiveness. Good agreement was achieved between the theoretical and experimental variations of rotor effectiveness with nondimensional flow rate for both seals.

The main conclusions are:

- In general, not all the ingested hot gas that enters the rim-seal clearance can penetrate into the wheel-space, and enthalpy can be exchanged even if no ingested fluid enters the wheel-space.
- An equation has been derived to account for both ingress and frictional heating on the adiabatic rotor effectiveness. It is shown that the superposed cooling flow acts as a buffer to reduce the effect of ingress on the rotor temperature, and when $\Psi = 1$ there is a critical flow rate above which ingress has no effect on the temperature; this buffer effect increases as the sealing effectiveness of the rim seal decreases.
- An equation has also been derived to account for both ingress and frictional heating on the adiabatic rotor temperature. In particular, it is shown that not only is the rotor temperature increased directly by the local shear stress it is also increased indirectly by the work done by the rotor on the entrained fluid that is recirculated via the stator boundary layer.
- In gas turbines, the increase of rotor temperature due to the direct frictional heating can be as high as 40C, which can have a significant effect on the life of this expensive component. The buffer effect helps to offset the adverse effects of both ingress and the indirect frictional heating.

The model and equations derived in this paper are of direct use to the designers of the internal-air systems of gas turbines.

REFERENCES

[1] Sangan, C.M., Lalwani, Y., Owen, J.M. and Lock, G.D., 2013, "Experimental Measurements of Ingestion Through Turbine Rim Seals: Part 5—Fluid Dynamics of Wheel-Space," ASME Paper GT2013-94148.

[2] Scobie, J. A., Sangan, C. M., Owen, J. M. and Lock, G. D., 2016, "Review of Ingress in Gas Turbines," ASME J. Eng. Gas Turbines & Power, 138 (12), 120801.

[3] Chew, J.W., Green, T., and Turner, A.B., 1994, "Rim Sealing of Rotor-Stator Wheelspaces in the Presence of External Flow," ASME Paper 94-GT-126.

[4] Pountney, O. J., Sangan, C. M., Lock, G. D., and Owen, J. M., 2013, "Effect of Ingestion on Temperature of Turbine Disks." ASME J. Turbomach. 135(5), 051010.

[5] Cho, G., Sangan, C. M., Owen, J. M. and Lock, G. D., 2016, "Effect of Ingress on Turbine Discs," ASME J. Eng. Gas Turbines & Power, 138, 042502.

[6] Mear, L. I., Owen, J. M. and Lock, G. D., 2016, "Theoretical Model to Determine Effect of Ingress on Turbine Disks," ASME J. Eng. Gas Turbines & Power, 138, 032502.

[7] Tian, S., Zhang, Y. and Su, W., 2014, "Effects of Gas-Ingestion through Turbine Rim Seals on Flow and Heat Transfer in the Wheel-space," ASME Paper GT2014-26635.

[8] Childs, P.R.N., 2011, "Rotating Flow," Elsevier: Oxford, UK.

[9] Mear-Stone, L., 2015, "Theoretical Modelling of Flow in Rotor-Stator Systems," PhD thesis, University of Bath.

[10] Owen, J.M., 2011, "Prediction of Ingestion through Turbine Rim Seals—Part I: Rotationally Induced Ingress," ASME J.Turbomach., , 133(3), p.031005.

[11] Owen, J.M., 2011, "Prediction of Ingestion through Turbine Rim Seals—Part II: Externally Induced and Combined Ingress," ASME J.Turbomach., 133(3), p.031006.

[12] White, F.M., 2011, "Fluid mechanics," McGraw-Hill, New York, USA.

[13] Sangan, C. M., Pountney, O. J., Zhou, K., Wilson, M., Owen, J. M., and Lock, G. D., 2011, "Experimental Measurements of Ingestion through Turbine Rim Seals—Part II: Rotationally-Induced Ingress," ASME J. Turbomach., 135(2), p. 021013.

[14] Owen, J. M. and Rogers, R. H., 1989, "Flow and Heat Transfer in Rotating-Disc Systems, Volume 1: Rotor-Stator Systems", Research Studies Press, Taunton, UK; John Wiley, N.Y.

APPENDIX A: CALCULATION OF WORK TERM, W_r^*

W_r^*, the work done by the rotor on the fluid between $r = a$ and $r = b$, is given by

$$W_r^* = M^* \Omega \tag{A1}$$

where M^* is the frictional moment on the rotor. The moment coefficient C_M^* is defined by

$$C_M^* \stackrel{\text{def}}{=} \frac{M^*}{\frac{1}{2}\rho\Omega^2 b^5} \tag{A2}$$

so that

$$M^* = \frac{1}{2}\rho\Omega^2 b^5 C_M^* \tag{A3}$$

It follows that

$$\frac{W_r^*}{\dot{m}_o(H_i - H_o)} = C_M^* \frac{\mathrm{Re}_\phi}{C_{w,o}} \frac{\Omega^2 b^2}{2(H_i - H_o)} \tag{A4}$$

where Re_ϕ and $C_{w,o}$ are defined in the Nomenclature.

It was shown by Owen and Rogers [14] that

$$C_M^* = e_M \mathrm{Re}_\phi^{-0.2} \tag{A5}$$

where e_M is a constant that depends on the swirl ratio, β. For a free disc, where β = 0 and a = 0, e_M= 0.0729 . Eq (A4) can therefore be approximated by

$$\frac{W_r^*}{\dot{m}_o(H_i - H_o)} = \frac{e_M}{\lambda_{T,o}} \frac{\Omega^2 b^2}{2(H_i - H_o)} \tag{A6}$$

where $\lambda_{T,o}$ is defined in the Nomenclature.

APPENDIX B: RELATIONSHIP BETWEEN $\varepsilon_{H'}$ AND ε_{ad}

The definition of ε_{ad} is written here as

$$\varepsilon_{ad} \stackrel{\text{def}}{=} \frac{T_{r,ad} - T_{i,t}}{\tilde{T}_{ad,r} - T_{i,t}} \tag{B1}$$

where $T_{i,t}$ is the total temperature of the flow in the annulus and $\tilde{T}_{ad,r}$ is the adiabatic wall temperature when there is no ingress. Therefore

$$\tilde{T}_{ad,r} = T_{o,t} + \delta T \tag{B2}$$

where $T_{o,t}$ is the total temperature of the sealing air and δT is the temperature difference caused by frictional heating. This was calculated by Cho et al. by

$$\delta T \stackrel{\text{def}}{=} \frac{R\Omega^2 r^2}{2c_p}(1 - \beta)^2 < 1C \tag{B3}$$

As $H_i < H_o$ in the experiments, it is convenient to rewrite the definition of ε_H as

$$\varepsilon_H \stackrel{\text{def}}{=} \frac{H_r - H_i}{H_o - H_i} \tag{B4}$$

where

$$H_i = c_p T_{i,t} \tag{B5a}$$

$$H_o = c_p T_{o,t} \tag{B5b}$$

$$H_r = c_p T_{r,ad} + \frac{1}{2}\Omega^2 r^2 \tag{B5c}$$

Consequently, ε_{ad} can be related to ε_H by

$$\varepsilon_{ad} = \frac{\varepsilon_H - \dfrac{\Omega^2 r^2}{2(H_o - H_i)}}{1 + \dfrac{c_p \delta T}{H_o - H_i}} \tag{B6}$$

Eq. (4.26) is rewritten as

$$\varepsilon_H = \varepsilon_{H'} + \varepsilon_{c,s}(1 - \Psi)\frac{e_M}{\lambda_{T,o}}\frac{\Omega^2 b^2}{2(H_o - H_i)} + \frac{\Omega^2 r^2}{2(H_o - H_i)}[R(1-\beta)^2 + (1-\beta^2)] \tag{B7}$$

Therefore, eq (B6) can be rewritten as

$$\varepsilon_{ad} = \frac{\varepsilon_{H'} + \dfrac{c_p \delta T}{H_o - H_i} + \varepsilon_{c,s}(1 - \Psi)\dfrac{e_M}{\lambda_{T,o}}\dfrac{\Omega^2 b^2}{2(H_o - H_i)} - \dfrac{\beta^2 \Omega^2 r^2}{2(H_o - H_i)}}{1 + \dfrac{c_p \delta T}{H_o - H_i}} \tag{B8}$$

For convenience, define

$$\delta_1 \overset{\text{def}}{=} \frac{c_p \delta T}{H_o - H_i} \tag{B9a}$$

$$\delta_2 \overset{\text{def}}{=} \varepsilon_{c,s}(1 - \Psi)\frac{e_M}{\lambda_{T,o}}\frac{\Omega^2 b^2}{2(H_o - H_i)} \tag{B9b}$$

$$\delta_3 \overset{\text{def}}{=} \frac{\beta^2 \Omega^2 r^2}{2(H_o - H_i)} \tag{B9c}$$

Therefore

$$\varepsilon_{ad} = \frac{\varepsilon_{H'} + \delta_1 + \delta_2 - \delta_3}{1 + \delta_1} \approx \varepsilon_{H'} + (1 - \varepsilon_{H'})\delta_1 + \delta_2 - \delta_3 \tag{B10}$$

When $\Phi_o = \Phi_{\text{crit}}, \Psi = \varepsilon_{H'} = 1$, and $\delta_2 = 0$, so that

$$\varepsilon_{ad} \approx \varepsilon_{H'} - \delta_3 \tag{B11}$$

where

$$\delta_3 = \frac{\beta^2 \Omega^2 r^2}{2(H_o - H_i)} < 0.01 \tag{B12}$$

As $\varepsilon_{H'} = 0$ when $\Phi_o = 0$, and - as eq (B3) shows - $\delta T < 1C$, and so the differences for $0 < \Phi_o < \Phi_{crit}$ are expected to be relatively small.

Seal	Φ_{min}	Γ_c	A	B	$\Phi_{o,crit}$
Axial-clearance	0.200	0.644	1.21	47.1	0.143
Radial-clearance	0.121	2.01	1.21	47.1	0.143

Table 1: Correlation constants for $\varepsilon_{c,s}$& $\varepsilon_{H',r}$

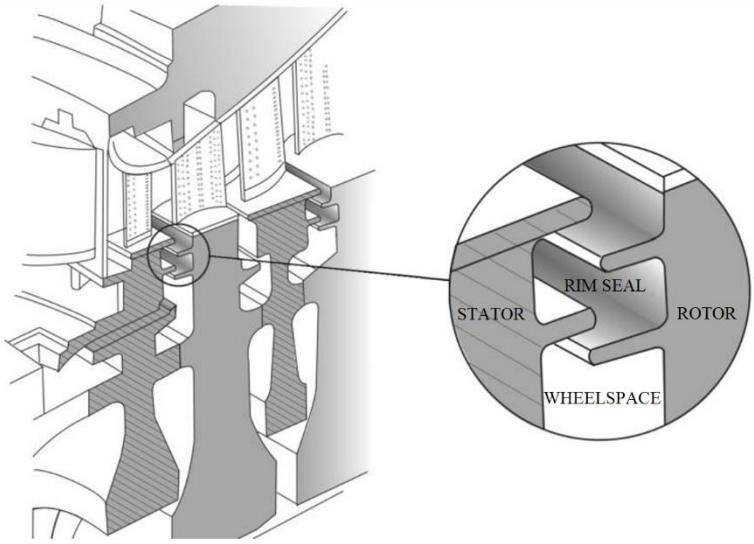

Fig. 1: Generic rotor-stator turbine stage, showing rim seal [1]

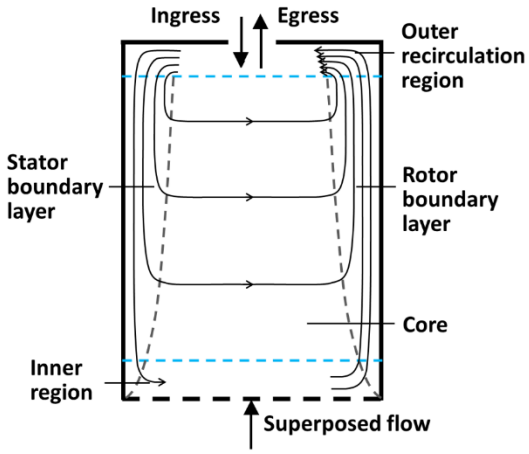

Fig. 2: Simplified model of flow structure in wheel-space

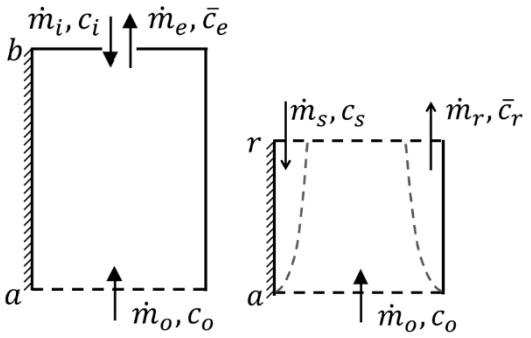

Fig. 3 (a): Outer control volume **Fig. 3 (b): Inner control volume**

Fig. 3: Control volumes for concentration

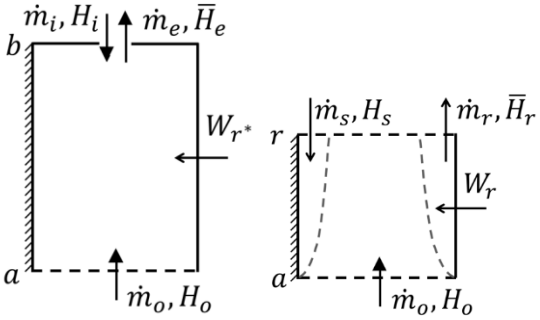

Fig. 4 (a): Outer control volume **Fig. 4 (b): Inner control volume**

Fig.4: Control volumes for enthalpy

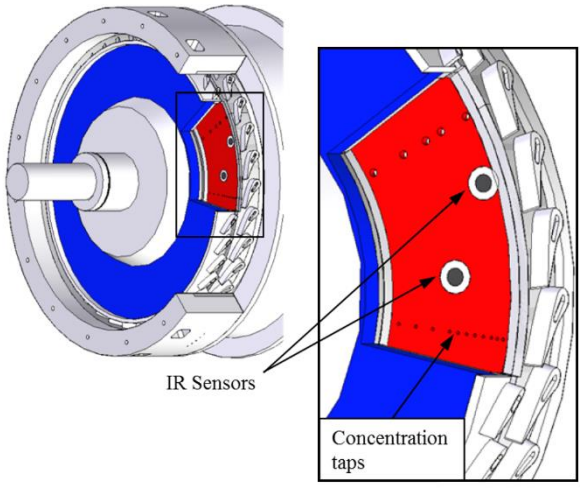

Fig. 5: Test section showing instrumentation in wheel-space (red, stationary; blue, rotating) [5]

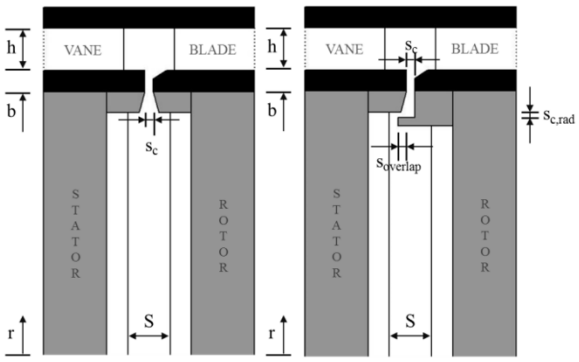

Fig. 6: Rim-seal configurations [5]

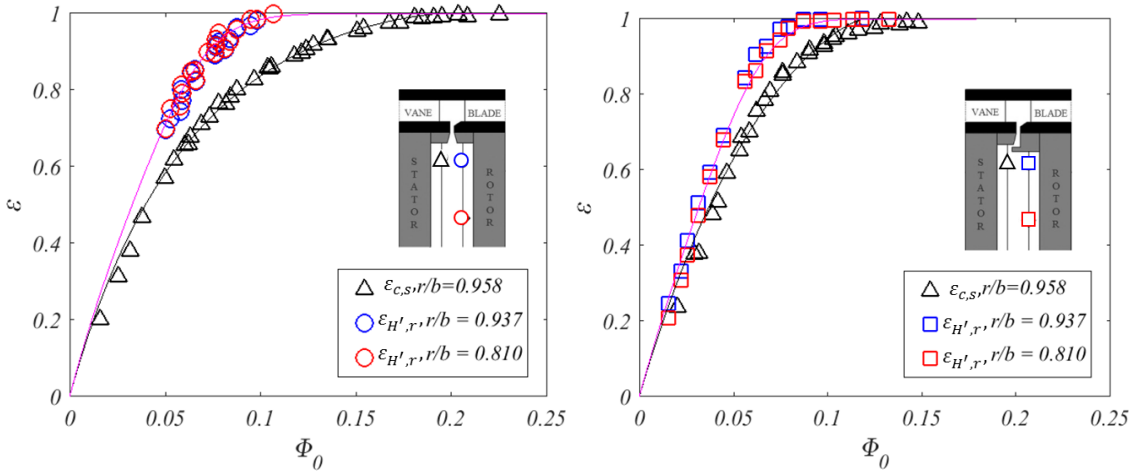

Fig.7 (a): Axial-clearance seal **Fig.7 (b): Radial-clearance seal**

Fig.7: Variation of $\varepsilon_{c,s}$& $\varepsilon_{H',r}$ with Φ_0. (Symbols denote experimental data [5]; curves show theoretical correlations.)

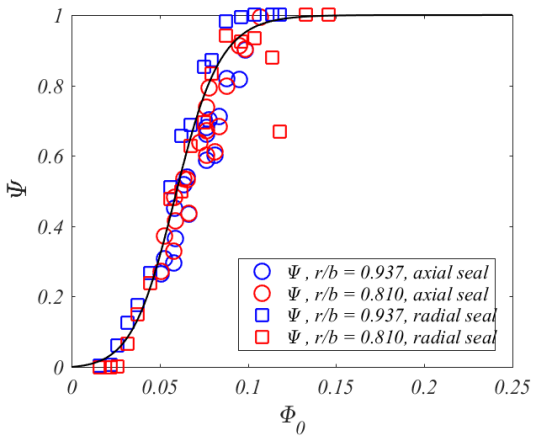

Fig. 8: Variation of Ψ with Φ_0. (Symbols denote experimental data [5]; curve show theoretical correlation.)